IEEE Access
Multidisciplinary | Rapid Review | Open Access Journal

Received 14 December 2023, accepted 22 January 2024, date of publication 21 February 2024, date of current version 26 March 2024.

Digital Object Identifier 10.1109/ACCESS.2024.3359756

RESEARCH ARTICLE

Lane-Changing Decision Intention Prediction of Surrounding Drivers for Intelligent Driving

PENGFEI TAO[1], XINGHAO REN[1], CONG WU[2], CHUANCHAO ZHANG[1], AND HAITAO LI[1]
[1]School of Transportation, Jilin University, Changchun 130022, China
[2]Hefei University of Technology Design Institute (Group) Company Ltd., Hefei 230601, China

Corresponding author: Haitao Li (lihait@jlu.edu.cn)

This work was supported by the Key Program of the National Natural Science Foundation of China under Grant 52131202.

ABSTRACT In complex traffic environment, it is still a great challenge for Autonomous Vehicles (AVs) to understand the surrounding drivers' Lane-Changing Decision (LCD) intention accurately. The LCD intention is affected by Driver's Psychology (DP) and Driving Style (DS). But few LCD studies considered DP and DS simultaneously. We previously proposed a LCD model, by combing DP and DS, termed as DP&DS-LCD model. Nevertheless, there are some factors not fully considered in this model, including the driver's Visual Attention (VA) in DP quantification and the influence of driving state on DS. Therefore, an enhanced LCD Model is developed, by integrating the DP under VA (DPVA) and DS Layering (DSL), named as DPVA&DSL-LCD model. In the model, a psychological field model coupling driver's VA mechanism is established to represent the surrounding vehicles' influence on the driver. Then, a DSL framework is proposed by adding the influence of driving state on DS. The Gaussian Mixture Model (GMM) clustering and Support Vector Machine (SVM) classifier are respectively adopted in training and recognition phases to identify the current driving style. Finally, integrating the DPVA and DSL, the Light Gradient Boosting Machine (LightGBM) algorithm is used to train the LCD model. In experiments, the open I-80 database from Next Generation Simulation (NGSIM) is adopted to train the DPVA&DSL-LCD. And compared with other three LCD models, the prediction performance of DPVA&DSL-LCD model achieved the best. Therefore, the DPVA&DSL-LCD model is effective and could provide support for the decision-making of AVs by predicting surrounding vehicles' LCD intention.

INDEX TERMS Autonomous vehicles, driver's psychology, driving state, driving style, lane change decision intention, visual attention mechanism.

I. INTRODUCTION

With the development and gradual application of intelligent driving technology, in the future, the Automatic Vehicles (AVs) and artificial vehicles will drive together. Due to the AVs could not understand the driving intention of surrounding artificial vehicles accurately, so that the AVs may make irrational behavior decisions. This may produce negative impact on the traffic operation safety. In order to solve this problem, it is necessary to predict the driving intention of the surrounding vehicles effectively, so as to optimize the control strategy of A.Vs.

Lane-Changing (LC) is a relatively high risky behavior in daily driving. Generally speaking, LC process includes LC Decision (LCD) and LC implementation stage. And this paper mainly studies the LCD process. According to the LC purpose, LCD behavior could be divided into Discretionary LCD (DLCD) and Mandatory LCD (MLCD) behavior. And the DLCD is addressed in this paper. During the LCD process, surrounding traffic environment stimulates the driver, which will lead to the change of Driver's Psychology (DP). Drivers may make discrepant LCD strategies under different psychological states. Meanwhile, the Driving Style (DS) will affect driver's LCD strategy. Therefore, in order to describe driver's LCD behavior, it is necessary to consider both the DP and DS. Driving style refers to the driver's personal driving ways with specific driving behavior characteristics displayed in different driving environments [45]. Driver's psychology usually refers to the psychological state and characteristics that affect the driver's cognition, emotion, and

The associate editor coordinating the review of this manuscript and approving it for publication was Christian Esposito.

behavior during driving. This includes, but is not limited to, aspects such as the driver's attention sharing, risk perception, decision-making, stress management, and emotional control. This article focuses more on the driver's visual attention and decision-making level.

Driving style and driving psychology are two different concepts, and we consider them to be important factors in the process of lane changing decision, and together with the current traffic conditions, road conditions, the performance of the vehicle itself, environmental factors, etc., determine the lane changing decision (LCD)

The driving style is a summary of the driving modes based on the driver's historical driving behavior habits and the characteristics of the vehicle's spatio-temporal trajectory. However, driving psychology is based on the psychological change characteristics of drivers in different specific traffic scenarios extracted from traffic psychology and other disciplines, which is a statistical feature of psychological activities generated by the audio-visual feedback mechanism of ordinary drivers. Specifically, the psychological changes of drivers lead to changes in driving styles. There are differences in the focus and distribution of attention of drivers with different driving styles to the surrounding vehicles, and there are also differences in the choice of driving strategies for similar traffic scenarios under the influence of this.

In the process of driving, the driver will be affected by many factors, such as: road traffic conditions, surrounding vehicles, the overall state of the driver, etc. These influencing factors may affect the driver's psychology, and under the influence of the driver's psychology, there may be a temporary change in the driver's behavioral characteristics, that is, the driver's driving style changes. As a result, the driver's style has a short-term time-varying characteristic. In addition to driving style, traffic contextual information can also impact driver's LC intent. For example, drivers' glance durations can increase by 0.25 s on average (a 20% increase) in the driving situation with an overtaking vehicle engaged, compared to that with no traffic [47].

Yifan Zhang et al. integrates the relevant human factors to design a new DLC decision-making model, which takes driving styles of surrounding vehicles into consideration and makes lane-change/keep decisions. However, it doesn't take driver's real-time visual attention characteristics into account, also doesn't classify and quantify the psychological characteristics of drivers. Yunchao Zhang et al. proposes a personalized risk lane-changing prediction framework that considers driving style and develops a dynamic clustering method to determine the best identification time window and methods of driving style. The time-window labeling (TWL) method provides a way to label data, however, it does not consider the discrepancy among drivers that would impact the labeling results due to the diversity of driving styles. Then, Li [14] proposed a gaze-based labeling method by monitoring a driver's gaze behavior, instead of using a time-window labeling method. They also propose a lane-change Bayesian network incorporated with a Gaussian mixture model to estimate a driver's lane-changing intent considering a driver's driving style over varying scenarios. However, it ignores the change of driver's real-time psychology.

So far, many LCD models have been proposed, such as rule-based [1], [2], [3], fuzzy logic-based [4], [5], [6], and data-driven LCD models [7], [8], [9], [10]. However, most researches concentrated on the objective LC conditions, and lacked of the consideration of human factors. To solve the above problems, our research group previously proposed a novel human-like LCD model by coupling DP and DS, named as DP&DS-LCD model [11]. The driver's psychological field theory is used to represent the psychological effect of surrounding vehicles on the driver. And the vehicle trajectory data are used to divide the driving styles. The DP&DS-LCD model can extract the driver's mental state and driving style while performing LCD, and provide support for AVs' LCD behavior.

In [46], for example, researchers utilized driver's eye gaze signal as the indicator to predict driver's LC intent. They segmented and labeled viewing zones into several areas, called area of interests (AOI), by tags of windscreen, left-side window, left view mirror, speedometer, and rear view mirror, etc. The labeled time-series AOI data were then collected using eye-tracking devices and fed into the intent estimation model.

However, the DP&DS-LCD model may exist some idealized factors in modeling the DP and DS. Firstly, DP&DS-LCD model assumed that the driver could observe all the contours of surrounding vehicles when quantifying the DP effect of surrounding vehicles on the driver. Nevertheless, driver's visual attention range is narrower with the speed increasing. Meanwhile, driver's attention distribution coefficient to surrounding vehicles are different while changing lanes. Secondly, the driving style is not invariable and affected by driver's current state [12], [13]. Therefore, we proposed an improved DP (driver's psychology) quantification method, which is based on driver's real-time visual attention characteristics. Also we established a real-time DSL (driving style layering) recognition model, which considers DP (driver's psychology) and DS (driving style) simultaneously.

In order to solve the above problems, a more authentic human-like LCD model is proposed in this paper. The improved model integrates the DP under Visual Attention (DPVA) and DS Layering (DSL), named as DPVA&DSL-LCD. Firstly, based on the real-time VA mechanism, an enhanced DP model is developed, which considers the driver's effective visual attention range and visual attention difference. Secondly, for distinguishing the driving styles under different driving states effectively, a real-time DSL recognition framework is designed. The framework includes the offline training and online recognition stage. And each stage includes the driving state and driving style training and recognition layer.

Additionally, the Vehicle-to-Vehicle (V2V) communication technology makes it possible to obtain the vehicles' trajectories in real time. As shown in Fig. 1, in V2V environment, it is available to obtain the trajectory data of surrounding vehicles in real time. Then, the LCD model is utilized to judge whether the surrounding vehicles are going to perform LC. If the surrounding vehicles have the LCD intention, it is necessary to provide alarm for AVs.

The rest of the paper is arranged as follows: section II reviews the related works about LCD models; section III gives the details of DPVA&DSL-LCD model, which includes the improved quantified expression of the DP pressure with psychological field model, DSL recognition framework, and LCD prediction; section IV discusses and analyzes the experimental results; section V is the summary of the article and discussion.

The main contributions of this research are as follows:

1) An improved DP quantification method is proposed, which is based on driver's real-time visual attention characteristics.

2) A real-time DSL recognition model is established. This framework considers the influence of driving state on driving style.

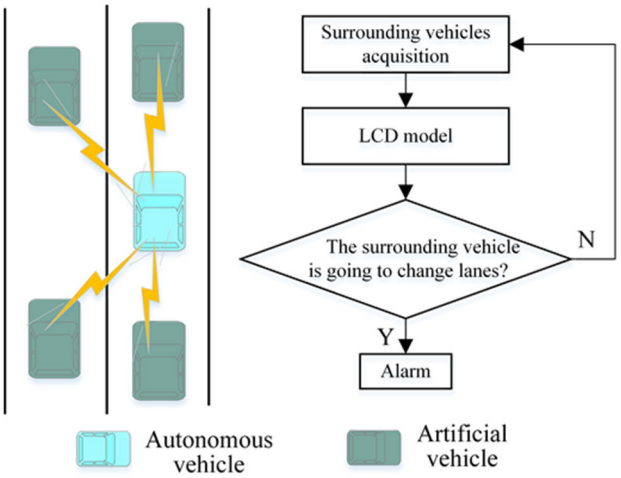

FIGURE 1. Framework of LC alarm system for AVs.

II. RELATED WORKS

So far, many LCD models have been developed. And the current LCD researches could be divided into three categories: rules-based, fuzzy logical, and data-driven model.

The rule-based LCD model established a set of LC rules to predict vehicle's LCD behavior. Gipps [1] firstly put forward a rule-based model which considered six factors: safe distance, the location of permanent obstructions, the presence of transit lanes, the intended turning movement of the driver, the presence of heavy vehicles, and the speed of the vehicle. Kind and Kesting [2] considered the lane utility and LC risk, and developed a general LCD model MOBIL (Minimizing Overall Braking Induced by Lane Changes). Wang et al.412 [3] based on the safety of AVs, developed a set of LC rules. And the reinforcement learning method is utilized in model training.

However, deterministic LC rules may ignore the uncertainty of driver perception. In order to solve this problem, the LCD models based on fuzzy logic were presented. The fuzzy logic model could deal with the uncertain relation in driving decision better, which consists of several if-then rules. For example, Das and Bowles [4] proposed a gap acceptance model based on the fuzzy logic, which mainly considered the speed and distance of LV and FV in the target lane, and the target vehicle's speed. Balal et al. [5] fuzzed the LC gap, and mainly considered the gap between the host vehicle and the LV (FV) in target lane, and the LV in present lane.

With the emergence of big data and intelligent algorithms, it provides the possibility for data-driven LCD models. There is no specific formula for the data-driven LCD model, which learns the characteristics through a large amount of LCD samples. Yuan et al. [8] selected the distance between the vehicle and the lane line, the longitudinal velocity, and lateral velocity of the vehicle as the input of LCD model. And in training and test phase, the Hidden Markov Model (HMM) is adopted. Zhang et al. [9] considered the location of six surrounding vehicles and the target vehicle while modeling LCD. And in training phase, they proposed a Hybrid Retraining Constraint (HRC) training to optimize the Long Short Term Memory (LSTM) algorithm. Xie et al. [10] selected the speed and location information of the target vehicle and surrounding three vehicles (LV and FV in target lane, and LV in current lane) as model input. Then, the Depth Belief Network (DBN) is adopted to train the LCD model. Wei et al. [36] proposed a prediction model based on the attention-assisted decoding decoder structure and deep neural network (DNN) to provide fine-grained predictions for the lane changing trajectories of intelligent connected cars and autonomous vehicles.

Although the above LCD models are based on different modeling methods, they are similar in quantifying the impact of the surrounding traffic conditions on the driver. The current LCD models mostly selected the objective traffic environment at the LCD time-point as the model input, which is a transient response model. However, the LCD process is a continuous decision process. The external traffic environment stimulates the driver, which will lead to the change of driver's mental state.

Meanwhile, different drivers may make disparate LCD strategies under the similar psychological states. And some studies have taken the driving style into the LCD model. Li et al. [14] used questionnaire survey to get the driver's driving style, and then added the driving style into LC intention model. The results showed that the prediction accuracy improved significantly after adding driving style. However, this is different from our work. Because our method does not need manually define the driving style, and all driver styles are learned from trajectory data. Ren et al. [15] took the velocity and acceleration of the target vehicle, the distance

between the target vehicle and LV, and LV's velocity as feature vectors. Then K-means algorithm is used to divide driving styles into three categories. In LC prediction, the Artificial Neural Network (ANN) is adopted. Xinpeng et al. [38] and others improved the DDPG algorithm and designed a smart car driving decision-making system to learn different styles of personalized driving strategies and form an improved personalized driving decision-making learning algorithm. Woo et al. [16] described the driving style based on the vehicles' car-following (CF) behavior. Then, the gap acceptance model is used to predict the LC behavior. Huan-Huan et al. [39] proposed a multi-attribute lane-changing decision model using the entropy weight method that introduced driving style, and analyzed the impact of driving style on the probability of lane-changing motivation and the probability of lane-changing success.

Additionally, there are many driving style classification methods. It could be roughly divided into two categories, the questionnaire survey based on the multi-dimensional driving style scale [17], [18] and the objective classification method based on vehicle trajectory data [19], [20], [21], [22], [23]. For example, Deng et al. [22] selected speed, acceleration, overspeed times, steering wheel angle and other vehicle performance indicators as the initial evaluation indexes of driving style. Then, the Principal Component Analysis (PCA) and K-means are adopted to divided the drivers into three categories. Wang et al. [23] chose speed, lateral acceleration, relative speed and following distance as the evaluation criteria of driving style. Then, they proposed a relative entropy method based on grid to quantify the similarity between extracted features, so as to classify drivers. Li and Liu [37] used a deep reinforcement learning (RL) approach is applied to design human-like agents for automated lane change decision considering the personalized preferences of different drivers.

The above two methods considered that, once the driver's style is obtained, it will not change. However, in driving process, the drivers will be influenced by many factors, such as road traffic condition, surrounding vehicles, driver's state, and etc. Under the effect of these comprehensive factors, driver's behavior characteristics may appear short change. In other words, the driving style presented by the driver changes. Therefore, driver's style exists the characteristics of short-term time variation. In order to obtain the driving style characteristics under different traffic scenarios, compared with the historical trajectory data, the real-time trajectory data could reflect the driver's present style more accurately. Additionally, because the driver's style is affected by the current state, it is necessary to classify the driving style on the basis of driving state recognition.

To solve the above problems, based on the previously developed DP&DS-LCD model, an enhanced LCD model is developed. The improved LCD model considers the DP under VA mechanism and the DSL, named as DPVA&DSL-LCD model. And the detailed modeling process is shown in the section III.

III. DPVA AND DSL-LCD MODEL

The DPVA&DSL-LCD model mainly contains three parts, as shown in Fig. 2. Firstly, based on the visual attention mechanism, an enhanced psychological field model is used to quantify the DP. It includes the definition of the driver's psychological field, the effect area of psychological field, and the DP calculation method under visual attention characteristic. Then, in order to get the driver's current driving style, a DSL system is proposed. The DSL definition framework considers the influence of driving state on the driving style. It includes the offline training module and the online interference module. Each module consists of two sub-modules, they are driving state and driving style module. Finally, the DPVA and the DS are used for LCD prediction. And the Light Gradient Boosting Machine (LightGBM) algorithm is adopted to train the model.

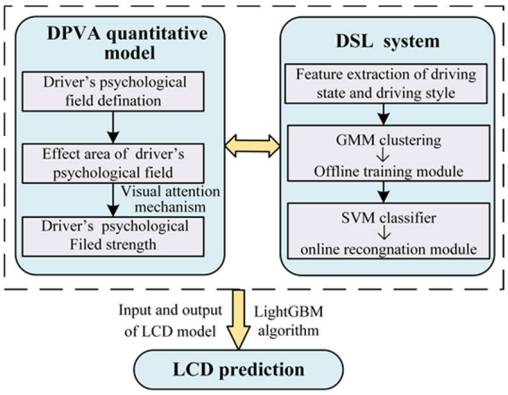

FIGURE 2. Framework of DPVA&DSL-LCD model.

A. DP QUANTITATIVE METHOD BASED ON VISUAL ATTENTION MECHANISM IN DPVA&DSL-LCD MODEL

The external traffic environment will stimulate the driver's senses, which will lead to the change of the driver's psychological state and affect the LCD behavior. Therefore, in order to accurately predict driver's LCD behaviors under different external traffic situations, it is necessary to quantify the psychological pressure of surrounding traffic environment on the driver.

In this paper, driver's psychological field theory and the visual attention mechanism are adopted to quantify the driver's mental state. The driver's psychological field model used the ''field theory'', and abstracted the surrounding traffic circumstances on the driver's psychological stimulation to a mental field. The psychological field source is the driver, and the effect area of the psychological field is determined by the driver's attention to the surrounding traffic environment and the visual attention range. By calculating the sum of the psychological pressure in the effect area of psychological field, the total mental field intensity could be obtained.

1) DRIVER'S PSYCHOLOGICAL FIELD MODEL

The driver's psychological field model [24] proposed by our research group is used to quantify the driver's psychological

states. In the model, the surrounding traffic environment on the driver's psychological effects is abstracted to a field model. By taking the expanded time distance as the basis of the strength and weakness distribution of the field strength, the driver's mental field distribution is mathematically described.

The basic field strength represents the psychological pressure of a certain point surrounding the driver, and it is closely related to the time distance from this point to the target vehicle. The smaller the time distance between the point and the target vehicle, the greater the psychological pressure (field strength) generated by the driver. Therefore, there is the negative correlation between the two variables. The basic field strength can be expressed as:

$$eb_i = \frac{v_i + v_\varepsilon}{d_0} \tag{1}$$

Here, v_i is the speed of target vehicle, v_ε is the speed correction. d_0 is the projected distance between the point and the target vehicle in the moving direction of the target vehicle.

The construction of the equipotential line mainly refers to the previous research [24]. Since the field strength of any position on the equipotential line is the same, the equivalent distance of the point in the moving direction of the target vehicle can be calculated, as (2) shown.

$$d_0 = \frac{d_{(x,y)}}{1 - (1-\alpha)\,|\sin\theta|} \tag{2}$$

Here, $d_{(x,y)}$ is the distance between any point and the origin (the driver's position). α is the ratio of the distance between the point where the equipotential line intersects the vehicle's moving direction and the origin, and the distance between the point where the equipotential line intersects the direction perpendicular to the vehicle's moving direction and the origin. θ is the angle between the line which is from any point on the equipotential line to the origin and the vehicle's running direction.

Based on (1) and (2), the basic field strength of any point in the driver's psychological field, as (3) shown.

$$eb_i = \frac{v_i + v_\varepsilon}{d_{(x,y)}}\left[1 - (1-\alpha)\,|\sin\theta|\right] \tag{3}$$

2) THE CALCULATED METHOD FOR THE PSYCHOLOGICAL EFFECT OF THE VEHICLES IN THE PSYCHOLOGICAL FIELD ON THE DRIVER

While performing LC, the safe LC gap is needed to find on the current and target lane. Therefore, the driver's attention is on the vehicles in the current lane and target lane, as shown in Fig. 3 (take the left LC as an example). The closer the surrounding vehicles are to the driver, the greater psychological influence on the driver, that is, the greater the field strength. The field strength displays the tendency of centering on the driver and gradually weakening around.

However, the driver's attentions on surrounding vehicles (vehicle$n+1, n+2, n-2$ in Fig. 3) are discrepant. Generally speaking, the driver pays more attention to the target lane than

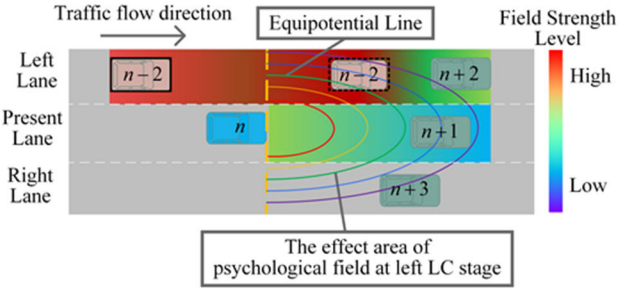

FIGURE 3. Illustration of driver's psychological field. Here "n" denotes the host vehicle. "n+1" denotes the LV on the present lane. "n-2" and "n+2" respectively denote the LV and FV on the left lane. "n+3" denotes the LV on the right lane.

the current lane when changing lanes. And for the target lane, the focus on the FV (vehicle$n-2$) exceeds that on the LV (vehicle$n+2$). The unbalanced attention distribution to lanes determines the unbalanced distribution of field strength.

Taking surrounding vehicle j as an example, the psychological pressure caused by the car to the driver could be calculated. As demonstrated in Fig. 4, suppose that the unilateral visual attention angle of driver i at time t is φ^t (the blue shaded area in Fig. 4). In general, if the vehicle's speed is low, the driver's visual attention field will be large, and the complete contour of surrounding vehicle j could be observed, they are Q_1Q_2 and Q_2Q_3. And let the driver's visual attention angle be φ^t_{ideal} in ideal conditions.

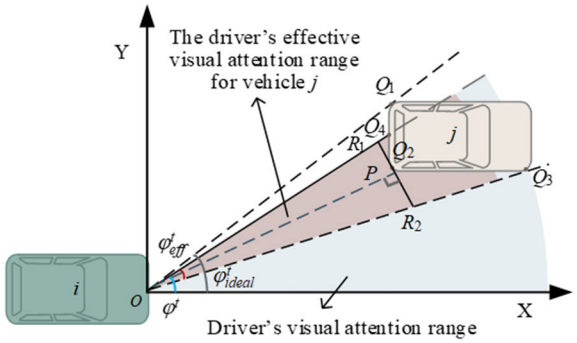

FIGURE 4. Driver's effective visual attention range for surrounding vehicle j based on the visual attention mechanism.

Nevertheless, when the vehicle is running at a high speed, the visual attention range will decrease rapidly [25]. The driver may only see partial outline of vehicle j. Suppose that the intersection point between the edge line of visual attention field and vehicle j is Q_4. That is, the driver's actual perceived contour for vehicle j are Q_4Q_2 and Q_2Q_3, which are actually the visual projection line R_1R_2 in driver's eyes. Let φ^t_{eff} represents the effective visual perception angle for vehicle j (the red shaded area in Fig. 4).

The calculation method of φ^t_{eff} is as follows:

$$\varphi^t_{eff} = \begin{cases} 0, & if\ \varphi^t \le h_{OQ_3} \\ \varphi^t - h_{OQ_3}, & if\ h_{OQ_3} < \varphi^t < h_{OQ_1} \\ \varphi^t_{ideal}, & if\ \varphi^t \ge h_{OQ_1} \end{cases} \tag{4}$$

where, h_{OQ_3} is the angle between line OQ_3 and the driving direction of the target vehicle i. And h_{OQ_1} is the angle between line OQ_1 and the driving direction of the target vehicle i. The φ^t_{ideal} satisfies $\varphi^t_{ideal} = \angle Q_1 O Q_3$.

Set the coordinates of R_1 and R_2 are (x_1, y_1) and (x_2, y_2), then the equation of the line R_1R_2 is:

$$\begin{cases} x = \lambda \\ y = \dfrac{y_2 - y_1}{x_2 - x_1}\lambda + \dfrac{y_1 x_2 - y_2 x_1}{x_2 - x_1} \end{cases} \tag{5}$$

Each point on the line R_1R_2 has a basic field, so the first curve integral is adopted to calculate the field intensity. Then, the mental field strength of vehicle j on the driver at time t is calculated as:

$$\begin{aligned} e^t_{ij} &= \int_{R_1R_2} eb_i(x, y)ds \\ &= \int_{x_1}^{x_2} eb_i\left(\lambda, \frac{y_2 - y_1}{x_2 - x_1}(\lambda - x_1) + y_1\right)\sqrt{1 + \left(\frac{y_2 - y_1}{x_2 - x_1}\right)^2}\, d\lambda \end{aligned} \tag{6}$$

Let $\frac{y_2 - y_1}{x_2 - x_1} = h$, $\frac{y_1 x_2 - y_2 x_1}{x_2 - x_1} = b$, combining with (3), the (6) can be simplified as:

$$e^t_{ij} = (v_i + v_\varepsilon)\sqrt{h^2 + 1}\left\{\begin{array}{l} \int_{x_1}^{x_2} \frac{1}{\sqrt{\lambda^2 + (h\lambda + b)^2}} d\lambda \\ -(1 - \alpha)\int_{x_1}^{x_2} \frac{|h\lambda + b|}{\lambda^2 + (h\lambda + b)^2} d\lambda \end{array}\right\} \tag{7}$$

here, when R_1R_2 is above the $X - axis$, $|h\lambda + b| = h\lambda + b$; when R_1R_2 is below the $X - axis$, $|h\lambda + b| = -h\lambda - b$ $|h\lambda + b| = -h\lambda - b$. Particularly, if R_1R_2 intersects to the $X - axis$, the intersection point will be set as $R_3(x_3, y_3)$, then e^t_{ij} is:

$$\begin{aligned} e^t_{ij} &= (v_i + v_\varepsilon)\sqrt{h^2 + 1} \\ &\times \left\{\begin{array}{l} \int_{x_1}^{x_3} \frac{1}{\sqrt{\lambda^2 + (h\lambda + b)^2}} d\lambda + \int_{x_3}^{x_2} \frac{1}{\sqrt{\lambda^2 + (h\lambda + b)^2}} d\lambda \\ -(1 - \alpha)\int_{x_1}^{x_3} \frac{h\lambda + b}{\lambda^2 + (h\lambda + b)^2} d\lambda \\ +(1 - \alpha)\int_{x_3}^{x_2} \frac{h\lambda + b}{\lambda^2 + (h\lambda + b)^2} d\lambda \end{array}\right\} \end{aligned} \tag{8}$$

Attention, the (7) and (8) are valid on the premise of $x_1 < x_2$. For other cases, it could be derived easily.

As mentioned before, there are differences in driver's attentions to vehicles in the scope of psychological field. The driver's attention distribution coefficient to the surrounding vehicle j is assumed to be ω^t_{ij}. In conclusion, the driver's total field intensity e^t_i can be expressed as:

$$e^t_i = \sum_{j \in eS^t_i} \omega^t_{ij} \times e^t_{ij} \tag{9}$$

Here, eS^t_i is the effect scope of psychological field of driver i at time t.

B. DSL MODEL

Marina Martinez et al. [12] pointed out that driving style is influenced by external environment (such as traffic conditions, weather, road type, and etc.) and internal human factors (such as age, gender, driving state, and etc.). And Eboli et al. [13] proved the influence of driving state on driving style through experiments. This paper mainly focuses on the influence of the driver's state on the driving style. And in order to accurately obtain the driving style, it is necessary to divide the driving style under the same driving state. The following consists of two parts: the feature vector construction of driving state and driving style, and the overall classification framework. Ying-Shi et al. [40] and others built a multi-modal automatic driving behavior prediction model based on the attention mechanism to accurately predict the steering wheel angle and vehicle speed, thereby predicting the driver's next driving behavior.

1) FEATURE VECTOR CONSTRUCTION OF DRIVING STATE AND DRIVING STYLE

a: DRIVING STATE

The driving state could be reflected by the vehicle's driving conditions and the driver's response characteristic to surrounding stimulation. The speed, acceleration, following distance, and Reaction Time (RT) are selected to describe the driving state, that are:

$$f_1 = \{v, a, gap, RT\} \tag{10}$$

where, v and a are the vehicle's speed and acceleration. gap is the distance between the target vehicle and the LV in current lane.

RT is the time interval between the driver's awareness of the motion state change with the LV, and the specific actions (acceleration or deceleration). Olson and Dewar [26] pointed out that RT was composed of four parts: detection, estimation, decision making and movement.

As for the remarking methods of RT, the graphical method is adopted. This method considers that the stimulation source is the speed or distance difference between the FV and LV, and the final effect of stimulation is the change of FV's speed or acceleration [27], [28]. And RT is the peak time-point difference between the relative velocity curve of LV and FV, and FV's acceleration curve.

The concentration degree of driving state is reflected in the vehicle's driving stability. Previous studies have pointed out that when driver is in distracted state, the speed will decrease, the following distance will increase, and the speed and following distance presented great fluctuation [29]. For speed and acceleration, the Coefficient of Variation (CV) is selected to measure the driving stability. Generally speaking, the smaller the CV of speed and acceleration are, the more concentrated the driver is. As for the following distance and RT, the average value is adopted. The more concentrated the driver is, the shorter RT to the surrounding vehicles is, and the smaller the following distance is [30].

Additionally, although the driver's driving state is influenced by surrounding environment, it is still stable in a certain time period. This paper assumes that the driver's state remains stable within the time length of T_1, and the value of T_1 is recommended from 3s to 5s. The final feature vector of driving state is showed in Table 1.

TABLE 1. The feature vector of driving state.

Evaluation index category	Index name	Statistical feature
Vehicle running condition	v, a	CV
	gap	Mean
Driver characteristics	RT	Mean

where, $CV = \sigma / \bar{x}$. σ is the Standard Deviation (SD), and $\bar{x}$ is the average value.

b: DRIVING STYLE

The focus of this paper is the driving style while changing lanes. When the driver wants to execute LC, the driver usually needs to consider the safe LC factors between target vehicle and the LV on the current lane and the LV and FV on the target lane. The more aggressive the driver is, the more likely he/she is to change lanes with risk.

For the target vehicle and the LV on the current lane, there is rear-end risk. Therefore, the safe Time HeadWay (THW) is adopted to quantify this risk. And there is lateral collisions risk between the host vehicle and the LV (FV) in target lane. In previous studies, Time to Collision (TTC) was used to quantify this risk. TTC is the time required to crash for the two vehicles if they are running at the current speed on the road.

However, TTC has certain limitations. It only considers the relative speed of the two vehicles, but ignores the vehicles' acceleration. However, it is difficult for vehicles to maintain uniform motion. Therefore, Ozbay et al. [31] proposed a Modified TTC (MTTC) model which considers both the relative velocity and the relative acceleration, as (11) and (12) shown.

Case 1: if $\Delta a \neq 0$

$$MTTC = \begin{cases} t_1, & if\ (t_1 < t_2, t_1 > 0\ and\ t_2 > 0)\ \ OR \\ & if\ \ (t_1 > 0\ and\ t_2 \leq 0) \\ t_2, & if\ (t_1 \geq t_2, t_1 > 0\ and\ t_2 > 0)\ \ OR \\ & if\ \ (t_1 \leq 0\ and\ t_2 > 0) \end{cases} \tag{11}$$

where,

$$t_1 = \frac{-\Delta v - \sqrt{\Delta v^2 + 2\Delta a \times d}}{\Delta a}$$

$$t_2 = \frac{-\Delta v + \sqrt{\Delta v^2 + 2\Delta a \times d}}{\Delta a}$$

Case 2: if $\Delta a = 0$ and $\Delta v > 0$

$$MTTC = TTC = \frac{d}{\Delta v} \tag{12}$$

In (11) and (12), Δv and Δa are the relative speed and relative acceleration between vehicle n and vehicle $n+2$ $(n-2)$. d is the distance between vehicle n and vehicle $n+2$ $(n-2)$.

The final driving style evaluation index is:

$$f_2 = \left\{THW, MTTC_{n,n+2}, MTTC_{n,n-2}\right\} \tag{13}$$

where, THW is the time headway between the host vehicle and the LV in the current lane, which satisfies $THW = d_{n,n+1}/v$, $d_{n,n+1}$ is the distance between vehicle n and vehicle $n+1$. v is the speed of target vehicle. $MTTC_{n,n+2}$ $(MTTC_{n,n-2})$ is the improved TTC between the target vehicle n and the LV $n+2$ (FV $n-2$) on the target lane.

The following is the feature vector of driving style. And the focus of the study is the LC style. Let the t_{LCI} and t_{LCD} respectively represent the time of LC Intention (LCI) and LCD. The trajectory data from t_{LCI} to t_{LCD} are extracted as initial input. In the construction of driving style feature vector, the mean value of the evaluation index in LCD stage is mainly selected, as shown in (14).

$$f_3 = \left\{THW, MTTC_{n,n+2}, MTTC_{n,n-2}\right\}_{mean}^{t_{LCI}:t_{LCD}} \tag{14}$$

2) REAL-TIME DSL FRAMEWORK

Furthermore, based on the feature vector construction of driving state and driving style, a real-time and layered driving style classification framework is proposed, mainly including the offline training module and online inference module, as shown in Fig. 5. And each module includes driving state layer and driving style layer. In Fig. 5, the cluster number of driving state is set as K, where $K = 1, 2, \ldots k, \ldots$. And the G_k is the cluster number of driving style under k-th driving state.

Firstly, based on the V2V environment, the historical trajectory data of vehicles could be acquired and utilized in the offline training module. And the real-time upload trajectory data make it possible to identify the driving style online.

Offline training module is composed of driving state and driving style sub-modules. Driving state training module mainly uses historical trajectory data to extract the feature vector, and then adopts Gaussian Mixture Model (GMM) clustering to establish the mapping relationship between driving behavior characteristic and the driving state. Suppose that the driving states are divided into K categories. On the basis of driving state classification, the driving style is divided under the same driving behavior data to driving state and driving style can be obtained.

The general process of GMM clustering is as follows:

Input: Sample set $D = \{x_1, x_2, \ldots, x_i, \ldots, x_m\}$.

For the classification of driving status, $x_i = \{v_{cv}, a_{cv}, gap_{mean}, RT_{mean}\}^{t-T_1:t}$, The number of clusters is K, For the classification of driving styles, $x_i = \left\{THW, MTTC_{n,n+2}, MTTC_{n,n-2}\right\}^{t_{LCI}:t_{LCD}}$, The number of clusters is G_k, G_k is the number of clusters of driving styles in the k-th driving state.

Output: The classification label corresponding to the sample.

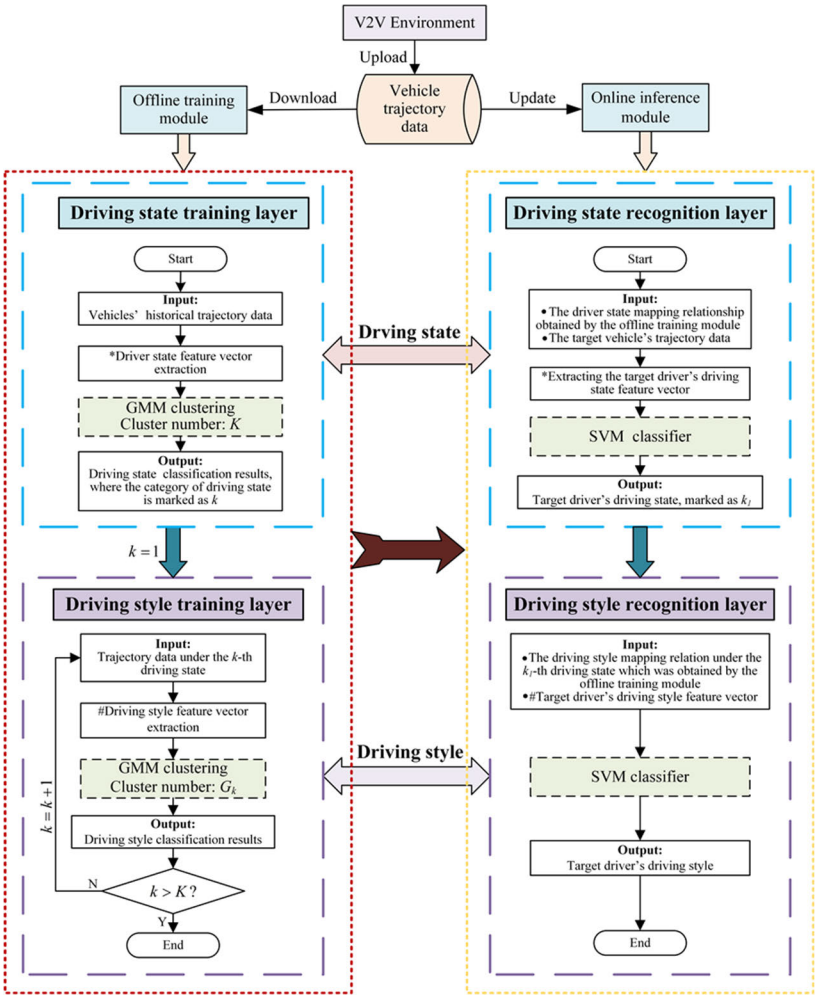

FIGURE 5. DSL recognition framework.

(1) Suppose the input samples obey a mixed Gaussian distribution, as shown in equations 15 and 16:

$$p(x) = \sum_{i=1}^{k} \alpha_i p(x|u_i, \sum i) \tag{15}$$

$$p(x|u_i, \sum i) = \frac{1}{(2\pi)^{n/2} \sum i^{1/2}} \times \exp\left\{-\frac{1}{2}(x-\mu_i)^T \sum i^{-1} (x-\mu_i)\right\} \tag{16}$$

In equation 2, α_i is the mixing coefficient, which represents the probability that the i-th Gaussian distribution is selected, satisfying $\sum_{i=1}^{k} \alpha_i = 1$; $p(x|u_i, \sum i)$ is the basic multivariate Gaussian distribution function; n is the dimension, the input vector x and the mean vector u_i are both n-dimensional vectors, and the covariance matrix $\sum i$ is an n-dimensional matrix.

(2) Initialize the model parameter α_i, μ_i and $\sum i$ of the mixed Gaussian distribution.

(3) The EM algorithm is used to update the model parameters:

$$u_i' = \frac{\sum_{j=1}^{m} \gamma_{ji} x_j}{\sum_{j=1}^{m} \gamma_{ji}} \tag{17}$$

$$\sum i' = \frac{\sum_{j=1}^{m} \gamma_{ji} (x_j - \mu_i')(x_j - \mu_i')^T}{\sum_{j=1}^{m} \gamma_{ji}} \tag{18}$$

$$\alpha_i' = \frac{\sum_{j=1}^{m} \gamma_{ji}}{m} \tag{19}$$

where γ_{ji} is the posterior probability of the observation data x_j generated by each mixed component, that is, the probability $p(z_j = i|x_j)$ of the observed data x_j generated by the i-th submodel, and the calculation method is shown in equation 20:

$$\gamma_{ji} = \frac{\alpha_i p(x_j|u_i, \sum i)}{\sum_{l=1}^{K} \alpha_l p(x_j|u_l, \sum l)} \tag{20}$$

(4) Repeat steps (3) and (4) until the iteration stop condition is met. The iteration stop criterion is generally $\left\|\theta_i^{t+1} - \theta_i^t\right\| \le \varepsilon$, where θ_i^{t+1} and θ_i^t are the parameter sets of

the i-th Gaussian distribution model at t+1 and t-th iterations respectively, satisfying $\theta_i^{t+1} = \left\{\alpha_i^{t+1},\ \mu_i^{t+1},\ \sum_i^{t+1}\right\}$ and $\theta_i^t = \left\{\alpha_i^t,\ \mu_i^t,\ \sum_i^t\right\}$, ε is a very small positive number.

(5) All samples are classified into the class to which they belong according to equation 21, that is, the higher the probability of which sub-model each sample comes from, it will be classified into the cluster. The result is class K, that is, $C = \{c_1, c_2, c_3, \ldots, c_k\}$.

$$\lambda_j = \underset{i=\{1,2,\ldots,k\}}{\arg\max}\ \gamma_{ji} \tag{21}$$

Based on the comparative experiments from the perspective of the model, three commonly used lane change decision models were compared, namely the Gipps model, the fuzzy inference model and the DBN model. The input variables for the three comparison models are shown below.

TABLE 2. Compare experimental model inputs.

Compare models	Model inputs
Gipps	$v,\ d_{n,n-2},\ d_{n,n+2},\ \Delta v_{n+2,n-2}$
Fuzzy logic	$d_{n,n+1},\ d_{n,n+2},\ d_{n,n-2},\ d_{n,n+2}+d_{n,n-2}$
DBN	$v,\ \Delta v_{n,n+1},\ \Delta v_{n,n+2},\ \Delta v_{n,n-2},\ d_{n,n+1},\ d_{n,n+2},\ d_{n,n-2}$

where, n is the main vehicle, $n+1$ is the front vehicle in the lane where the main vehicle is located, and $n+2$ and n-2 are the front and rear vehicles in the target lane, respectively. v is the velocity of the main vehicle. d_{ij} and Δv_{ij} are the distance and speed difference between vehicle i and vehicle j respectively. Δv_{ij} satisfies $\Delta v_{ij} = v_i - v_j$.

In order to verify the effectiveness of the prediction of lane change decision by integrating driver psychology and driving style, the LightGBM algorithm is used in the training stage only considering the different input variables of different models in the comparative experiment.

The online inference module could identify the driving style in real-time. Based on the mapping relationship obtained from the offline training module, the online inference module utilizes the real-time uploaded trajectory data to recognize the driving state and driving style. And the Support Vector Machine (SVM) algorithm is adopted to identify the driver's current driving state and driving style.

C. LCD BEHAVIOR PREDICTION

1) INPUT AND OUTPUT OF DPVA&DSL-LCD MODEL

The LCD process is from the LCI point to the LCD point. when extracting LCD data. And the driver's psychological field strength in LCD process is a time series with length T, and set it to E^t. The expression for E^t is defined as follows:

$$E^t = \left\{e^{t-T}, e^{t-T+\Delta t}, e^{t-T+2\Delta t}, \ldots, e^{t-\Delta t}, e^t\right\} \tag{22}$$

with

$$e^t = \sum_{j\in eS_i^t} \omega_{ij}^t \times e_{ij}^t = \sum_{j=n+1,n+2n-2} \omega_{ij}^t \times e_{ij}^t \tag{23}$$

here, Δt is the frequency of data acquisition, $\Delta t \in [0.01, 1]s$. "$n+1$" represents the front vehicle on the current lane, "$n+2$" and "$n-2$" are respectively the front and behind vehicle of the target lane.

There are differences in driver's psychological states between LCD and LK stages. In order to get the influence of driver's mental state on LCD, feature extraction is carried out on driver's mental state. Finally, four feature vectors are extracted, including the mean value and SD of E^t, the psychological field intensity at the LCD time-point (e^t), and the difference value between $\bar{E}^{t-\Delta t}$ and e^t.

Conclusively, combing the feature of driver's psychological state with driving style, the model input could be obtained, as (24) shown:

$$X = \left\{\bar{E}^t, (E^t)_{SD}, e^t, \bar{E}^{t-\Delta t} - e^t\right\} \tag{24}$$

And the model output is:

$$Y = \begin{cases} 0, & LK\ behavior \\ 1, & LCD\ behavior \end{cases} \tag{25}$$

2) LIGHTGBM ALGORITHM

The LightGBM algorithm [34] is adopted in the training stage of LCD model. LightGBM is an integrated learning method based on the decision tree classifier, which aims at the long training time of Gradient Boosting Decision Tree (GBDT) algorithm, and puts forward four improvement methods. They are histogram algorithm, Gradient-based One-Side Sampling (GOSS), Exclusive Feature Bundling (EFB), and leaf growth strategy. The optimized LightGBM algorithm has shorter training time and higher accuracy. And it is widely in classification and regression field. The specific optimization methods are as follows:

a: HISTOGRAM ALGORITHM

The basic idea of histogram algorithm is discretizing the continuous input eigenvalues into k discrete values, and construct the histogram with width k, as demonstrated in Fig. 6. Thus, it is not necessary to presort all the data when traversing the training data, only the cumulative statistics of each discrete value in the histogram are required. In feature selection phase, it is only needed to traverse to find the optimal segmentation point according to the discrete value of the histogram. The introduction of histogram algorithm greatly reduces the data storage space during model training, and accelerates the search speed of optimal segmentation points.

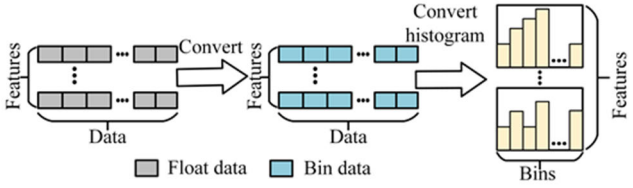

FIGURE 6. Schematic diagram of histogram algorithm.

Driver's LCI is subjective, and the LCI time-lengths of different drivers exist differences. The existing studies indicated that the time-length of drivers is distributed between 1s and 5s [32], [33]. Therefore, a sliding time-window T from 1s to 5s is adopted.

b: GOSS

The GOSS method considers that the data with larger gradient play a greater role in the calculation of information gain, and optimize the sampling efficiency of the training set. By sorting the absolute gradient values of the sample points in descending order, the sample points with large gradient are retained, and random sampling is carried out for the sample points with small gradient. Then, the two kinds of samples are combined to train a weak classifier. And a weight coefficient is added to the samples with small gradient when calculating the classifier gain.

c: EFB

The EFB method could reduce the feature dimensions by bundling exclusive features. And it can effectively improve the training efficiency of high-dimensional feature vectors.

d: LEAF-WISE GROWTH STRATEGY WITH MAP DEPTH RESTRICTION

As shown in Fig. 7, the leaf-wise growth strategy selects the leaf node with the highest information gain as the splitting point, and increases the maximum depth limitation of the number tree. Compared with level-wise strategy, the calculation cost of leaf-wise strategy is lower and the calculation result is more accurate.

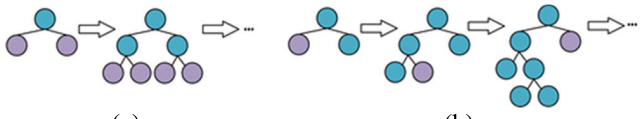

FIGURE 7. Diagram of decision tree's growth strategy. (a) Level-wise growth strategy; (b) Leaf-wise growth strategy.

IV. EXPERIMENTS

In order to demonstrate that the DPVA&DSL-LCD model is effective, the open Next Generation Simulation (NGSIM) date is used in the experiment. And this section contains three parts: database and data processing, model validation, and experiment results and analysis.

A. DATABASE AND DATA PROCESSING

The I-80 freeway dataset from open NGSIM database is adopted to learn and test the model. The vehicle trajectory data from lane 1 to lane 7 are collected. And the dataset includes three periods: from 4:00 p.m. to 4:15 p.m., from 5:00 p.m. to 5:15 p.m., and from 5:15 p.m. to 5:30 p.m. The data collection frequency is 0.1s. Before experiments, it is necessary to preprocess the original data to remove the influence of noise data on the experimental results. And the processing method is as follows:

(1) The LCD behavior of the passenger car is only studied. This is because the LCD factors of large vehicle and motorbike are different from the passenger car and the sample size is small.

(2) Only vehicle data from lane 2 to lane 6 are used. Since lane 1 is a high-occupancy lane, the vehicles' LC behavior on this lane are not considered. Because the lane 7 is near the entrance of the ramp and many vehicles are forced to change lanes. Moreover,

(3) The continuous LC data are excluded. Because any vehicle movement more than one lane is more likely a mandatory movement.

For the marking of LCD point, the most accurate method is to find the continuous change point of vehicle's lateral position. However, this method will take a long time when facing large amounts of data. Therefore, in order to label the LCD points quickly in real traffic situations, this paper adopted a simple method by referring to the existing studies. The study pointed out that the LCD point is: in the first 5 s before the vehicle's lane ID changing, when the lateral velocity is larger than 0.6m/s firstly [35]. And the LCD time-point is represented as t_{LCD}.

Then, based on the above LCI time-window, the LCD data are the trajectories from time $t_{LCD} - T$ to time t_{LCD}. Moreover, to ensure the LK trajectories and LCD trajectories have the same time length and in similar traffic conditions, the trajectories from time $t_{LCD} - 2T$ to time $t_{LCD} - T$ are labeled as LK samples. Finally, 972 LC samples and 856 LK samples are obtained.

B. MODEL VALIDATION

Model validation includes two parts, algorithm comparison and model comparison. The eXtreme Gradient Boosting (XGboost) algorithm [41] based on Bagging and Random Forest (RF) algorithm [42] based on Boosting are adopted in algorithm comparison. The model comparison part includes three LCD models, which are DP&DS-LCD model previously proposed by our research group, Gipps model [1], and fuzzy inference model [5]. In order to highlight the improvement of the DPVA&DSL-LCD model, only the input of the two comparison models are used for reference when testing Gipps model and fuzzy inference model.

In experiments, the data were randomly divided into training set and test set by the ratio of 7:3. True Positive Rate (TPR) and False Positive Rate (FPR) are used to evaluate the prediction performance. The two evaluation indexes are calculated by (26).

$$TPR = \frac{TP}{TP + FN}$$
$$FPR = \frac{TN}{FP + TN} \tag{26}$$

here TP, TN, FP, and FN are the true positive, true negative, false positive, and false negative. The LC and LK samples are respectively labeled as positive and negative samples.

Furthermore, the Area Under the Curve (AUC) index provided by Python editor is utilized to evaluate the overall performance of the binary classifiers. AUC value is the area under the Receiver Operating Characteristic (ROC) curve. Where, the ROC curve is the changing curve of TPR and FPR of the test set under different classification thresholds. The AUC value is between 0 and 1. The higher the AUC value, the better the prediction performance of model.

C. EXPERIMENT RESULTS AND ANALYSIS

The experimental results include two parts: driving style classification and LCD prediction results.

1) DRIVING STYLE CLASSIFICATION RESULTS

In the driving state classification stage, T_1 is set as 5s, that is, the trajectory data of 5 s before the time point of driving state recognition is selected as the initial input. Before classification, correlation analysis should be carried out on evaluation indicators to remove the influence of multicollinearity among indicators on evaluation results. In this paper, the Spearman coefficient is adopted, which is a parametric test method. The correlation analysis results are shown in Fig. 8. It can be found that, the absolute values of correlation coefficients among all indexes are less than 0.30. Therefore, the evaluation indexes of driving state and driving style display weak correlation, which could meet the evaluation requirements.

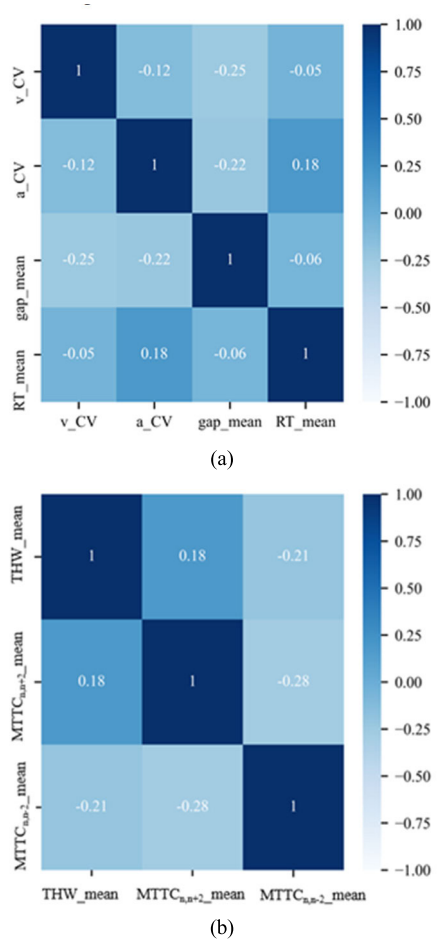

FIGURE 8. The evaluation index correlation analysis of driving state and driving style. (a) Driving state. Where, v_CV and a_CV are the CV of vehicle's speed and acceleration. gap_mean and RT_mean are the mean value of following distance and RT; (b) Driving style. Where, THW_mean, MTTCn,n+2_mean, and MTTCn,n+2_mean are respectively the mean value of THW, the MTTC between vehicle n and vehicle n+2, and the MTTC between vehicle n and vehicle n-2.

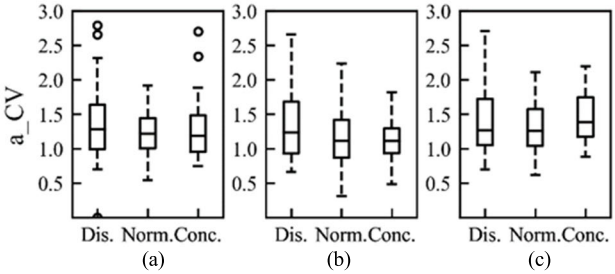

FIGURE 9. Boxplot of the CV of acceleration under different driving styles. Where, a_CV is the CV of acceleration. "Dis.", "Norm.", and "Conc." respectively represent distracted, normal, and concentrated driving state. (a) Cautious driver; (b) Neutral driver; (c) Aggressive driver.

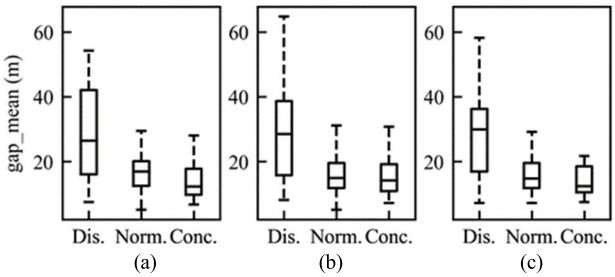

FIGURE 10. Boxplot of the mean gap under different driving styles. Where, gap_mean is the mean value of gap. "Dis.", "Norm.", and "Conc." respectively represent distracted, normal, and concentrated driving state. (a) Cautious driver; (b) Neutral driver; (c) Aggressive driver.

For the clustering number of driving state and driving style, they are set as 3. In addition, the CV of acceleration and the mean value of gap in each driving state under the same driving style are counted in this paper, as shown in Fig. 9 and Fig. 10. It can be found that, for the drivers with the same driving style, the more concentrated the driving state is, the less fluctuation of the acceleration is, and the smaller of the average following distance is.

In addition, Fig. 11 displays the distribution of average RT for the drivers with the same driving style in three driving states. Here, the vertical axis represents the driving state, and the horizontal axis represents the driving style. The Fig. 11 indicated that, for the same kind of driver, the driving state is more concentrated, the average RT distributes more centralized, and the shorter of RT.

The average MTTC distribution between the target vehicle n and the FV $n-2$ in the target lane under different driving styles are compared in this paper, as shown in Fig. 12. It can be found that, under the distracted driving state, the MTTC of cautious drivers are between 0.1 s and 2.4 s, and the MTTC of neutral and aggressive drivers are respectively from 0.1 s to

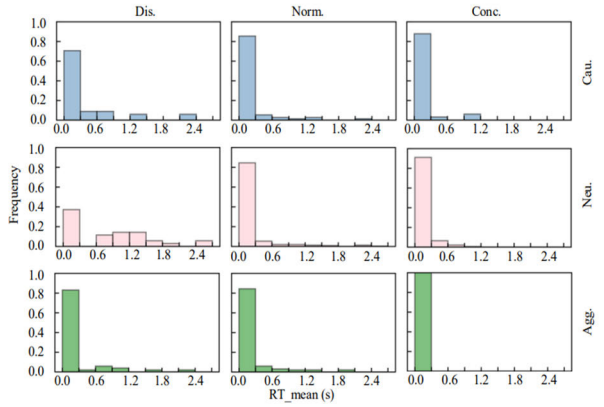

FIGURE 11. Frequency distribution histogram of the average RT under three driving states. Where, RT_mean is the average value of RT.

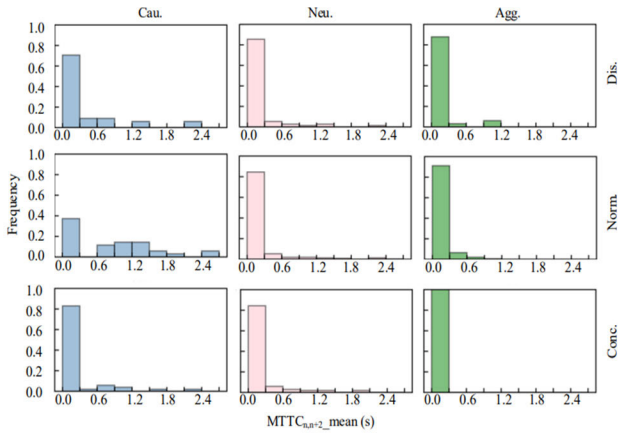

FIGURE 12. Frequency distribution histogram of average MTTC between the target vehicle n and the FV n-2 in the target lane under three driving styles. Where, MTTC$_{n,n-2}$_mean is the average value of MTTC$_{n,n-2}$.

1.5 s and from 0.1 s to 1.2 s. Although the MTTC difference between the cautious and neutral drivers is not distinct, the MTTC of the aggressive drivers is significantly lower than that of the other two types of drivers. Similarly, for the MTTC distribution in normal and concentrated driving states, it could get the similar conclusion with distracted driving state. That is, in the same driving state, the more aggressive drivers tend to change lanes at a shorter safe LC time.

2) PREDICTION RESULTS OF DPVA&DSL-LCD MODEL

The following assumptions are made in the calculation of driver's dynamic scope of visual attention:

(1) When the vehicle is moving forward, driver's visual field fixation point is the current driving direction;

(2) The driver's visual attention angle displays symmetrical distribution with the axis of view center line.

In previous studies, the relationship between the driver's visual attention range and the speed has been presented [23], as shown in Table 3, it can be found that: the driver's visual attention range is inversely proportional to the speed.

TABLE 3. Relationship between dynamic visual attention angle and speed.

Speed (km/h)	0	40	60	80	100	120
Visual attention angle (°)	170	100	86	60	40	22

Though Table 3 has given the relationship between some discrete speeds and the visual field angles, visual field angles at multiple specific speeds are needed in experiments.

Therefore, the linear regression is utilized to fit the visual attention angles and speeds, and the fitting results is shown in (27):

$$\varphi = -1.207^{*}\mathrm{v} + 160.1 \tag{27}$$

Meanwhile, it is difficult to obtain the driver's real-time eye movement data during the actual driving. Therefore, this paper simplified the attention coefficient of the driver for the surrounding vehicles in experiment, supposed that $\omega_{ij} = 1$.

a: ALGORITHM COMPARISON

Our experimental environment is under Windows server with two 3.0GHZ CPUs and 8G running memory. Table 4 shows the AUC values of the three algorithms under five time windows. Among them, the optimal AUC values of the same type driver under all time-windows are bold. It could get two conclusions from Table 4.

(1) Compared with the other two algorithms, DPVA&DSL-LCD has the best predictive performance. After driver classification, the AUC value of DPVA&DSL-LCD model is from 96.91% to 97.43%. The AUC of XGboost model is distributed between 91.51% and 93.58%. For RF model, the AUC value is from 89.88% to 92.63%.

(2) The prediction performance is significantly improved after driving style classification. The average AUC value of DPVA&DSL-LCD model improved by 2.77% after adding driving style. For XGboost and RF algorithm, the AUC respectively increased 0.87% and 1.12%.

The TPR and FPR values of different algorithms are shown in Fig. 13. Here, the vertical axis represents the driver style.

And the TPR and FPR values of each type of driver are the average values under the five time-window lengths. It could found that, for the three types of drivers, the overall predictive

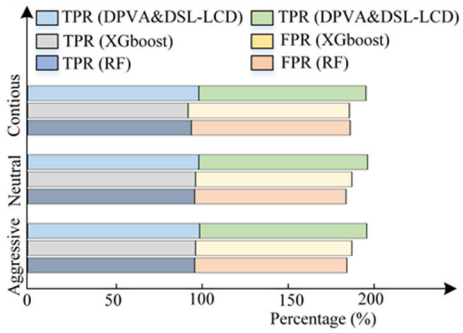

FIGURE 13. Stacked bar charts of different algorithms' TPR and FPR values.

TABLE 4. AUC performance of different algorithms (unit: %).

Driving Style	DPVA&DSL-LCD					XGboost					RF				
	1s	2s	3s	4s	5s	1s	2s	3s	4s	5s	1s	2s	3s	4s	5s
Cautious	96.88	96.97	96.88	**97.01**	96.92	91.43	90.62	92.86	**93.03**	92.46	90.42	92.89	**92.95**	92.74	92.83
Neutral	**97.89**	97.27	96.84	97.10	97.79	92.89	92.05	**93.52**	93.50	93.04	88.60	91.13	**92.38**	91.41	92.34
Aggressive	**97.51**	96.79	97.22	96.62	97.42	92.54	91.87	92.86	**94.19**	93.52	90.62	90.00	92.42	92.08	**92.72**
Mean	97.43	97.01	96.98	96.91	97.38	92.29	91.51	93.08	93.58	93.01	89.88	91.34	92.58	92.08	92.63
Non-Classified	93.96	95.27	93.70	93.16	**95.74**	91.64	89.96	**93.52**	92.06	91.98	90.39	90.36	**91.37**	90.75	90.05

performance of DPVA&DSL-LCD model is better than other two algorithms.

b: MODEL COMPARISON

Table 5 compares the AUC values of the four LCD models. Where, the AUC value for each type of driver is the average.

TABLE 5. AUC values of different LCD models (unit: %).

Driving Style	DPVA&DSL-LCD	DP&DS-LCD	Gipps	Fuzzy Reasoning
Cautious	96.93(SD=0.05)	94.23(SD=0.40)	58.00	71.31
Neutral	97.38(SD=0.40)	94.33(SD=1.18)	61.95	69.00
Aggressive	97.11(SD=0.35)	95.25(SD=1.02)	67.24	70.17
Mean	97.14(SD=0.31)	94.60(SD=0.46)	62.40	70.16
Non-Classified	94.37(SD=0.98)	91.03(SD=0.96)	59.37	67.14

AUC values under five sliding time-windows. From Table 5, it could found that, after adding the driving style into LCD model, the AUC values improved obviously, which verifies that considering the driving style is significant for LCD prediction. And the performance of DPVA&DSL-LCD model is significantly better than other three LCD models. The average AUC value of DPVA&DSL-LCD model is 97.14%, which improved 2.54% compared with DP&DS-LCD model. Compared with Gipps model and Fuzzy Interference model, the improvement effect is more significant.

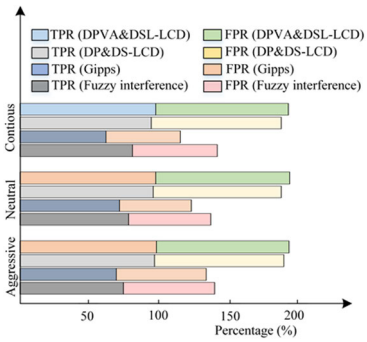

FIGURE 14. Stacked bar charts of different LCD models' TPR and FPR values.

Fig. 14 shows the prediction accuracy of LC and LK samples for the four LCD models. Here, the vertical axis represents the driver style. It indicates that compared with other three LCD models, the accuracy of DPVA&DSL-LCD model achieves the best, whether for LC samples or LK samples.

In conclusion, the DPVA&DSL-LCD model has achieved encouraging results. The average AUC value of DPVA&DSL-LCD model is 97.14%, and the average accuracy of LC and LK samples are respectively 98.27% and 95.94%. In addition, after adding the driver's current driving style into LCD model, the AUC value of the DPVA&DSL-LCD model increased from 94.37% to 97.14%. The results show that the prediction performance is significantly improved after taking into account the driver's visual attention mechanism quantification and driving style.

V. CONCLUSION AND DISCUSSION

For the current LCD models concentrated on the objective LC conditions, and lacked the consideration of DP and DS. So our research team previously proposed a novel LCD model, which coupled the DP and DS, and had encouraging predictive performance. But there are some idealization factors in DP modeling and DS classification. Therefore, we improved the previous DP&DS-LCD model. And the enhanced LCD model integrates the DP under Visual Attention (DPVA) and DS Layering (DSL), named as DPVA&DSL-LCD model. Firstly, in the DP quantitation, the enhanced DP model considers the visual attention range and the difference in attention distribution. Then, a DSL classification framework is developed, which considers the influence of driving state on driving style. After that, the LightGBM is adopted to train the DPVA&DSL-LCD model. The LightGBM algorithm is an integrated learning method with short training time and high prediction accuracy. Finally, the open I-80 dataset from NGSIM database is selected for model validation. The experimental results showed that after adding the real-time driving style into the LCD model, the LCD prediction performance improved effectively. And the DPVA&DSL-LCD model get better prediction results compared with the previous DP&DS-LCD model. Therefore, the DPVA&DSL-LCD model is verified to be more effective.

In conclusion, the DPVA&DSL-LCD model has achieved good predictive performance. However, due to the complexity of drivers' attention mechanism, the consideration of our research may not be very comprehensive. And in future studies, we will use eye tracker or other experimental equipment to quantify the attention distribution more detailed. So that the DP model will be conformer to the characteristics of drivers. And the final prediction results may be improved.

REFERENCES

[1] P. G. Gipps, "A model for the structure of lane-changing decisions," *Transp. Res. B, Methodol.*, vol. 20, no. 5, pp. 403–414, Oct. 1986.

[2] M. T. Kind and A. Kesting, "Modeling lane-changing decisions with MOBIL," in *Proc. 7th Int. Conf. Traff. Granul. Flow (TFG)*, Paris, France, Jun. 2007, pp. 211–221.

[3] J. Wang, Q. Zhang, D. Zhao, and Y. Chen, "Lane change decision-making through deep reinforcement learning with rule-based constraints," in *Proc. Int. Joint Conf. Neural Netw. (IJCNN)*, Jul. 2019, pp. 1–6.

[4] S. Das and B. A. Bowles, "Simulations of highway chaos using fuzzy logic," in *Proc. 18th Int. Conf. North Amer. Fuzzy Inf. Process. Soc.*, New York, NY, USA, Jun. 1999, pp. 130–133.

[5] E. Balal, R. L. Cheu, and T. Sarkodie-Gyan, "A binary decision model for discretionary lane changing move based on fuzzy inference system," *Transp. Res. C, Emerg. Technol.*, vol. 67, pp. 47–61, Jun. 2016.

[6] S. Moridpour, M. Sarvi, G. Rose, and E. Mazloumi, "Lane-changing decision model for heavy vehicle drivers," *J. Intell. Transp. Syst.*, vol. 16, no. 1, pp. 24–35, Jan. 2012.

[7] S. Coskun and R. Langari, "Predictive fuzzy Markov decision strategy for autonomous driving in highways," in *Proc. IEEE Conf. Control Technol. Appl. (CCTA)*, Copenhagen, Denmark, Aug. 2018, pp. 1032–1039.

[8] W. Yuan, Z. Li, and C. Wang, "Lane-change prediction method for adaptive cruise control system with hidden Markov model," *Adv. Mech. Eng.*, vol. 10, no. 9, Sep. 2018, Art. no. 168781401880293.

[9] X. Zhang, J. Sun, X. Qi, and J. Sun, "Simultaneous modeling of car-following and lane-changing behaviors using deep learning," *Transp. Res. C, Emerg. Technol.*, vol. 104, pp. 287–304, Jul. 2019.

[10] D.-F. Xie, Z.-Z. Fang, B. Jia, and Z. He, "A data-driven lane-changing model based on deep learning," *Transp. Res. C, Emerg. Technol.*, vol. 106, pp. 41–60, Sep. 2019.

[11] Z. Li, C. Wu, P. Tao, J. Tian, and L. Ma, "DP and DS-LCD: A new lane change decision model coupling driver's psychology and driving style," *IEEE Access*, vol. 8, pp. 132614–132624, 2020.

[12] C. M. Martinez, M. Heucke, F.-Y. Wang, B. Gao, and D. Cao, "Driving style recognition for intelligent vehicle control and advanced driver assistance: A survey," *IEEE Trans. Intell. Transp. Syst.*, vol. 19, no. 3, pp. 666–676, Mar. 2018.

[13] L. Eboli, G. Mazzulla, and G. Pungillo, "How drivers' characteristics can affect driving style," *Transp. Res. Proc.*, vol. 27, pp. 945–952, Feb. 2017.

[14] X. Li, W. Wang, and M. Roetting, "Estimating driver's lane-change intent considering driving style and contextual traffic," *IEEE Trans. Intell. Transp. Syst.*, vol. 20, no. 9, pp. 3258–3271, Sep. 2019.

[15] G. Ren, Y. Zhang, H. Liu, K. Zhang, and Y. Hu, "A new lane-changing model with consideration of driving style," *Int. J. Intell. Transp. Syst. Res.*, vol. 17, no. 3, pp. 181–189, Sep. 2019.

[16] H. Woo, Y. Ji, Y. Tamura, Y. Kuroda, T. Sugano, Y. Yamamoto, A. Yamashita, and H. Asama, "Lane-change detection based on individual driving style," *Adv. Robot.*, vol. 33, no. 20, pp. 1087–1098, Oct. 2019.

[17] S. G. Scott and R. A. Bruce, "Decision-making style: The development and assessment of a new measure," *Educ. Psychol. Meas.*, vol. 55, no. 5, pp. 818–831, Oct. 1995.

[18] O. Taubman-Ben-Ari, M. Mikulincer, and O. Gillath, "The multidimensional driving style inventory—Scale construct and validation," *Accident Anal. Prevention*, vol. 36, no. 3, pp. 323–332, May 2004.

[19] H. R. Eftekhari and M. Ghatee, "A similarity-based neuro-fuzzy modeling for driving behavior recognition applying fusion of smartphone sensors," *J. Intell. Transp. Syst.*, vol. 23, no. 1, pp. 72–83, Jan. 2019.

[20] Y. Feng, S. Pickering, E. Chappell, P. Iravani, and C. Brace, "Driving style analysis by classifying real-world data with support vector clustering," in *Proc. 3rd IEEE Int. Conf. Intell. Transp. Eng. (ICITE)*, Singapore, Sep. 2018, pp. 264–268.

[21] K.-T. Chen and H.-Y.-W. Chen, "Driving style clustering using naturalistic driving data," *Transp. Res. Rec., J. Transp. Res. Board*, vol. 2673, no. 6, pp. 176–188, Jun. 2019.

[22] Z. Deng, D. Chu, C. Wu, S. Liu, C. Sun, T. Liu, and D. Cao, "A probabilistic model for driving-style-recognition-enabled driver steering behaviors," *IEEE Trans. Syst., Man, Cybern., Syst.*, vol. 52, no. 3, pp. 1838–1851, Mar. 2022.

[23] W. Wang, W. Han, X. Na, J. Gong, and J. Xi, "A probabilistic approach to measuring driving behavior similarity with driving primitives," *IEEE Trans. Intell. Vehicles*, vol. 5, no. 1, pp. 127–138, Mar. 2020.

[24] P. Tao, "Modeling of driving behavior based on the psychology field theory," Ph.D. dissertation, School Transp., Jilin Univ., Changchun, China, 2012.

[25] B. Pan, Y. Zhao, and X. Liang, "Application of dynamic vision theory in highway alignment design," *J. Chang Univ., Natural Sci. Ed.*, vol. 6, pp. 20–24, Dec. 2004.

[26] P. Olson and R. Dewar, "Driver perception-response time," in *Human Factors in Traffic Safety*. Tucson, AZ, USA: Lawyers & Judges Publishing Company, 2002.

[27] G. S. Gurusinghe, T. Nakatsuji, Y. Azuta, P. Ranjitkar, and Y. Tanaboriboon, "Multiple car-following data with real-time kinematic global positioning system," *Transp. Res. Rec., J. Transp. Res. Board*, vol. 1802, no. 1, pp. 166–180, Jan. 2002.

[28] X. Zhang and G. H. Bham, "Estimation of driver reaction time from detailed vehicle trajectory data," in *Proc. 18th IASTED Int. Conf. Model. Simul.*, 2007, pp. 574–579.

[29] M. Wollmer, C. Blaschke, T. Schindl, B. Schuller, B. Farber, S. Mayer, and B. Trefflich, "Online driver distraction detection using long short-term memory," *IEEE Trans. Intell. Transp. Syst.*, vol. 12, no. 2, pp. 574–582, Jun. 2011.

[30] D. B. Kaber, Y. Liang, Y. Zhang, M. L. Rogers, and S. Gangakhedkar, "Driver performance effects of simultaneous visual and cognitive distraction and adaptation behavior," *Transp. Res. F, Traffic Psychol. Behaviour*, vol. 15, no. 5, pp. 491–501, Sep. 2012.

[31] K. Ozbay, H. Yang, B. Bartin, and S. Mudigonda, "Derivation and validation of new simulation-based surrogate safety measure," *Transp. Res. Rec., J. Transp. Res. Board*, vol. 2083, no. 1, pp. 105–113, Jan. 2008.

[32] E. Y. Chung, H. C. Jung, E. Chang, and I. S. Lee, "Vision based for lane change decision aid system," in *Proc. Int. Forum Strategic Technol.*, Ulsan, South Korea, Oct. 2006, pp. 10–13.

[33] N. Kauffmann, F. Winkler, F. Naujoks, and M. Vollrath, "'What makes a cooperative driver?' Identifying parameters of implicit and explicit forms of communication in a lane change scenario," *Transp. Res. F, Traffic Psychol. Behaviour*, vol. 58, pp. 1031–1042, Oct. 2018.

[34] G. Ke et al., "LightGBM: A highly efficient gradient boosting decision tree," in *Proc. Adv. Neural Inf. Process. Syst.*, vol. 2017, 2017, pp. 3147–3155.

[35] Y. Liu, X. Wang, L. Li, S. Cheng, and Z. Chen, "A novel lane change decision-making model of autonomous vehicle based on support vector machine," *IEEE Access*, vol. 7, pp. 26543–26550, 2019.

[36] C. Wei, F. Hui, Z. Yang, S. Jia, and A. J. Khattak, "Fine-grained highway autonomous vehicle lane-changing trajectory prediction based on a heuristic attention-aided encoder–decoder model," *Transp. Res. C, Emerg. Technol.*, vol. 140, Jul. 2022, Art. no. 103706.

[37] D. Li and A. Liu, "Personalized lane change decision algorithm using deep reinforcement learning approach," *Int. J. Speech Technol.*, vol. 53, no. 11, pp. 13192–13205, Jun. 2023.

[38] X. Wang, Z. Chen, C. Wu, and S. Xiong, "A method of automatic driving decision for smart car considering driving style," *J. Transport Inf. Saf.*, vol. 38, no. 2, pp. 37–46, 2020.

[39] F. Huan-Huan, D. Jian-Hua, and G. E. Ting, "Multi-attributes lane-changing decision model based on entropy weight with driving styles," *J. Transp. Syst. Eng. Inf. Technol.*, vol. 20, no. 2, pp. 139–144, 2020.

[40] G. Ying-Shi and H. Tao, "Multimodal autonomous driving-behavior prediction model based on attention mechanism," *China J. Highway Transport*, vol. 35, no. 9, pp. 141–156, Sep. 2022.

[41] Y. Zhang, X. Shi, S. Zhang, and A. Abraham, "A XGBoost-based lane change prediction on time series data using feature engineering for autopilot vehicles," *IEEE Trans. Intell. Transp. Syst.*, vol. 23, no. 10, pp. 19187–19200, Oct. 2022.

[42] Q. Sun, C. Wang, R. Fu, Y. Guo, W. Yuan, and Z. Li, "Lane change strategy analysis and recognition for intelligent driving systems based on random forest," *Expert Syst. Appl.*, vol. 186, Dec. 2021, Art. no. 115781.

[43] Y. Zhang, Q. Xu, J. Wang, K. Wu, Z. Zheng, and K. Lu, "A learning-based discretionary lane-change decision-making model with driving style awareness," *IEEE Trans. Intell. Transp. Syst.*, vol. 24, no. 1, pp. 68–78, Jan. 2023.

[44] Y. Zhang, Y. Chen, X. Gu, N. N. Sze, and J. Huang, "A proactive crash risk prediction framework for lane-changing behavior incorporating individual driving styles," *Accident Anal. Prevention*, vol. 188, Aug. 2023, Art. no. 107072.

[45] J. Reason, A. Manstead, S. Stradling, J. Baxter, and K. Campbell, "Errors and violations on the roads: A real distinction?" *Ergonomics*, vol. 33, nos. 10–11, pp. 1315–1332, Oct. 1990.
[46] F. Lethaus and J. Rataj, "Do eye movements reflect driving manoeuvres?" *IET Intell. Transp. Syst.*, vol. 1, no. 3, pp. 199–204, 2007.
[47] S. E. Lee, E. C. B. Olsen, and W. W. Wierwille, "A comprehensive examination of naturalistic lane-changes," Nat. Highway Traffic Saf. Admin., Washington, DC, USA, Tech. Rep. DOT HS 809 702, 2004.

PENGFEI TAO received the B.S. degree in computer science and technology and the M.S. and Ph.D. degrees in traffic engineering from Jilin University, China. He is currently an Associate Professor with the School of Transportation, Jilin University. His research interests include driving behavior analysis and autonomous vehicle.

XINGHAO REN received the bachelor's degree in traffic engineering from Jilin University, Changchun, China, in 2022, where he is currently pursuing the master's degree with the School of Transportation. His research interests include autonomous driving and driving decisions.

CONG WU received the master's degree from the School of Transportation, Jilin University, Changchun, China, in 2021. She is currently working with the Hefei University of Technology Design Institute(Group) Company, Hefei, China. Her research interests include traffic flow theory and driving behavior.

CHUANCHAO ZHANG received the bachelor's degree in traffic engineering from Changsha University of Science & Technology, in 2022. He is currently pursuing the master's degree with the School of Transportation, Jilin University. His research interest includes traffic safety.

HAITAO LI received the Ph.D. degree in traffic engineering from Jilin University, China, where he is currently pursuing the Ph.D. degree with the School of Transportation. His research interests include intelligent traffic control and traffic information processing.